INSTRUMENTATION FOR MICROWAVE REMOTE SENSING

M.Tech. Thesis

By
NARTHU SANTHOSH KUMAR

DEPARTMENT OF ASTRONOMY ASTROPHYSICS AND SPACE ENGINEERING
INDIAN INSTITUTE OF TECHNOLOGY INDORE
APRIL, 2023

INSTRUMENTATION FOR MICROWAVE REMOTE SENSING

A THESIS

Submitted in fulfillment of the
requirements for the award of the degree
of
Master of Technology

by

NARTHU SANTHOSH KUMAR

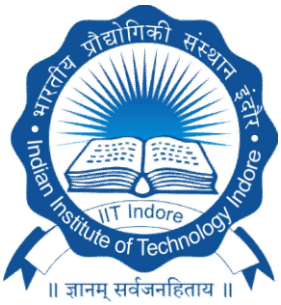

DEPARTMENT OF ASTRONOMY ASTROPHYSICS AND SPACE ENGINEERING
INDIAN INSTITUTE OF TECHNOLOGY INDORE
APRIL, 2023

INDIAN INSTITUTE OF TECHNOLOGY INDORE

CANDIDATE'S DECLARATION

I hereby certify that the work which is being presented in the thesis entitled **INSTRUMENTATION FOR MICROWAVE REMOTE SENSING** in the fulfillment of the requirements for the award of the degree of **MASTER OF TECHNOLOGY** and submitted in the **DEPARTMENT OF ASTRONOMY ASTROPHYSICS AND SPACE ENGINEERING, Indian Institute of Technology Indore**, is an authentic record of my own work carried out during the time period from June 2022 to April, 2023 under the supervision of Dr. Saurabh Das, Associate Professor, DAASE, IIT-Indore

The matter presented in this thesis has not been submitted by me for the award of any other degree of this or any other institute.

N. Santhosh Kumar
24/05/23

Signature of the student with date
(NARTHU SANTHOSH KUMMAR)

This is to certify that the above statement made by the candidate is correct to the best of my/our knowledge.

S. Das
24/05/2023

Signature of the Supervisor of
M.Tech. Thesis (with date)
(Dr. SAURABH DAS)

NARTHU SANTHOSH KUMAR has successfully given his/her M.Tech Oral Examination held on **25/04/2023**

S. Das

Convener, DPGC
Date: 24/05/2023

Signature of PSPC Member #1
(Prof. ABHIRUP DATTA)
Date: 31/05/2023

Saptarshi Ghosh

Signature of PSPC Member #2
(Dr. SAPTARSHI GOSH)
Date: 31/05/2023

ACKNOWLEDGEMENT

I wish to express my sincere thanks to my supervisor Dr. Saurabh Das for his humble and implicitly strict guidance, and timely suggestions. A special thanks to my fellow master's student Mr. Pushp Ranjan for his help in finding relevant literature, and handling the software/hardware components whenever needed in the support of developing one of the receiver systems. I am grateful to Mr. Subhanshu Umeshchandra Bishwash, Mr. Soumen Datta, and Ms. Hemapriya Raju for their help in testing the other receiver system. Also I am grateful to Mr. Harsha Avinash Tanti, Mr. Abhijeet Dutta for their help in transacting necessary components from RF lab. Finally, my sincere regards to the PSPC members Prof. Abhirup Datta, and Dr. Saptarshi Gosh for choosing to be responsible for my progress in Master's with a direct or indirect supervision in my final year thesis work

ABSTRACT

This Thesis reports my efforts put into devising or developing two different satellite-microwave receiver systems for use in remote sensing applications. One on the suggestion of my supervisor, and the other based on an opportunity found upon the literature review of a topic of my interest, which is Soil Health. First system is a SDR based receiver which can be used to receive microwave signals from any target satellite based on the operational frequency range of the SDR, and the second system is a GNSS based receiver meant to estimate the soil moisture content of a ground surface by utilizing the multi-path ground reflections of L-band signals transmitted by GNSS satellites.

TABLE OF CONTENTS

LIST OF FIGURES, TABLES

ACRONYMS

DC	Direct Current
dB	Decibels
FM	Frequency Modulation
GNSS	Global Navigation Satellite System
GNSS-R	GNSS-Reflectometry
GNSS-IR	GNSS-Interferometric Reflectometry
GPS	Global Positioning System
GSAT	Geostationary Satellite
IF	Intermediate Frequency
IIT	Indian Institute of Technology
ISRO	Indian Space Research Organization
LNB	Low Noise Block
L.O.	Local Oscillator
mAh	milliampere hour
OS	Operating System
PBO	Plate Boundary Observatory
PC	Personal Computer
RF	Radio Frequency
SD	Storage Drive

SDR	Software Defined Radio
SMA	Soil Moisture Content
SMAP	Soil Moisture Active Passive
SMA	Soil Moisture and Ocean Salinity
SNR	Signal to Noise Ratio
UNCCD	United Nations Convention to Combat Desertification
W	Watts

Chapter 1

Introduction

This chapter provides a very brief introduction to the microwave remote sensing, especially concerning to the soil moisture, and a brief overview of the Software Defined Radio(SDR), which two are the main components of my thesis

1.1 Introduction to Microwave Remote Sensing

Microwave remote sensing offers unique information on those aspects which can not be provided by other remote sensing techniques. Visible and infrared sensors, for instance, cannot detect the sea, wind, or wave direction, which are obtained from frequency characteristics, back-scattering, polarization, the Doppler effect, etc. which are specific to only microwaves. The following figure shows the relative position of the Microwave band with its designated sub-bands on the EM spectrum.

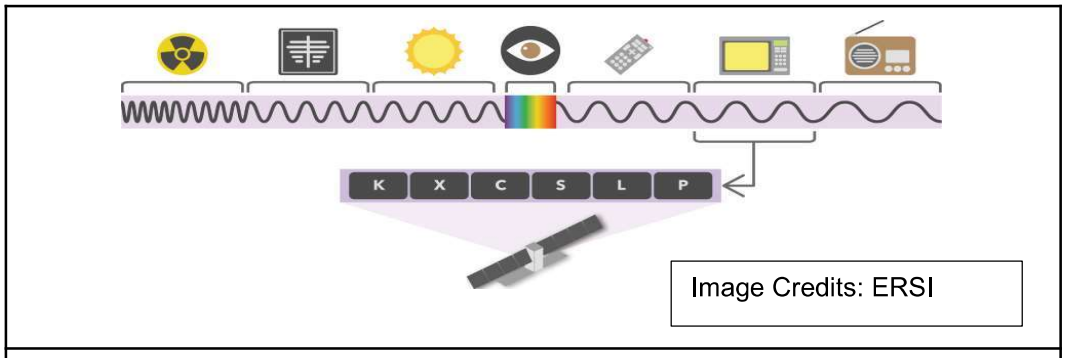

Fig-1.1 Microwave bands in EM spectrum

Frequently used microwave spectrum bands for remote sensing include the X-band, C-band, S-band, L-band, and P-band. Specific characteristics of each band can be found in the Table-0.1

Table-1.1

Band	**Frequency (GHz)**	**Wavelength (cm)**	**Key characteristics**
Ka	40–27	0.75–1.11	Usually for astronomical observations
K	27–18	1.11–1.67	Used for radar, satellite communications, astronomical observations, automotive radar
Ku	18–12	1.67–2.5	Typically used for satellite communications
X	12.5–8	2.4–3.75	Widely used for military reconnaissance, mapping and surveillance
C	4–8	3.75–7.5	Penetration capability of vegetation or solids is limited and restricted to the top layers. Useful for sea-ice surveillance
S	4–2	7.5–15	Used for medium-range meteorological applications, for example, rainfall measurement, airport surveillance
L	2–1	15–30	Penetrates vegetation to support observation applications over vegetated surfaces and for monitoring ice sheet and glacier dynamics, and very suitable for soil moisture monitoring
P	1–0.3	30–100	So far, only for research and experimental applications. Significant penetration capabilities

			regarding vegetation canopy, sea ice, soil, and glaciers

Microwave remote sensing is a powerful tool used in a variety of fields, including agriculture, hydrology, climate studies, and environmental monitoring. Some of the significant advantages of microwave remote sensing compared to other remote sensing techniques are:

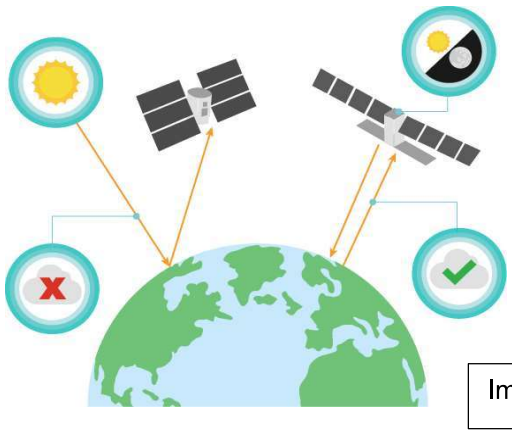

Fig-1.2 Optical versus Microwave remote sensing

1. Penetration of clouds and vegetation: Microwaves have a longer wavelength than visible light and can penetrate through clouds and vegetation. This allows for the observation of the Earth's surface even under cloudy or vegetated conditions, making microwave remote sensing useful for monitoring weather patterns, soil moisture, and vegetation health.
2. Sensitivity to water content: Microwaves are highly sensitive to the water content of a substance, making them an essential tool for measuring soil moisture, snow depth, and sea surface temperature. This sensitivity to water content is not found in other remote sensing techniques such as optical or infrared remote sensing.

3. Day and night observation: Unlike optical remote sensing, which relies on sunlight to illuminate the Earth's surface, microwave remote sensing can operate day or night, allowing for continuous monitoring of the Earth's surface. This is particularly important for applications such as weather forecasting and disaster management, where real-time information is crucial

1.1.1 Remote sensing for surface Soil Moisture

Soil across the globe is degrading at an alarming rate. According to the UNCCD 2020 report more than 50% of the world's soils, and more than 62% of India's soils are already degraded. Now it's of paramount importance to keep a constant eye on our soil health. Soil moisture plays an important role as a direct metric for soil health

Volumetric soil moisture, or the ratio of the volume of water to the volume of soil, is currently estimated using both in situ and remote sensing techniques. Unfortunately, in situ measurement methods are expensive and cumbersome over large areas. In the past two decades microwave remote sensing has proven successful for estimating dielectric properties of soil based on land surface emissivity leading to soil moisture estimation. Various low frequencies (X, C, and L bands) have typically been used to detect bare or vegetated soil surface moisture content. Several satellite-based L-band radiometers and radars including SMOS, AQUARIUS Ocean Salinity, and SMAP instruments are being used for global monitoring of near-surface (0–5 cm) soil moisture and ocean salinity.

Though all these traditional approaches are there to measure soil moisture, they fail in providing global coverage, and continuous observations in a cost-effective manner. GNSS-Reflectometry, emerging from last decade as a new method in Earth's surface remote sensing which mainly includes soil moisture sensing. And now it's having a huge global thrust because of its unique and various advantages

like: quick revisiting time, global coverage, low cost, all-weather, and near real-time when compared to conventional observations

1.2 Basic Concept of Software Defined Radio (SDR)

In simplest words SDR is like a sound card for RF signals with a support to a wide range of frequencies, modulation types, and signal characteristics with a single hardware platform with software-based digital signal processing to replace the traditional discrete hardware components used in radio communication systems. In traditional radio systems, most of the signal processing is performed by hardware components such as filters, amplifiers, mixers, and demodulators. The advantage of SDR is that it provides greater flexibility and adaptability compared to traditional systems. Since most of the signal processing is done in software, the SDR system can be reconfigured and updated using software rather than requiring hardware changes. Fig-1.3 shows the Basic Architecture of a SDR.

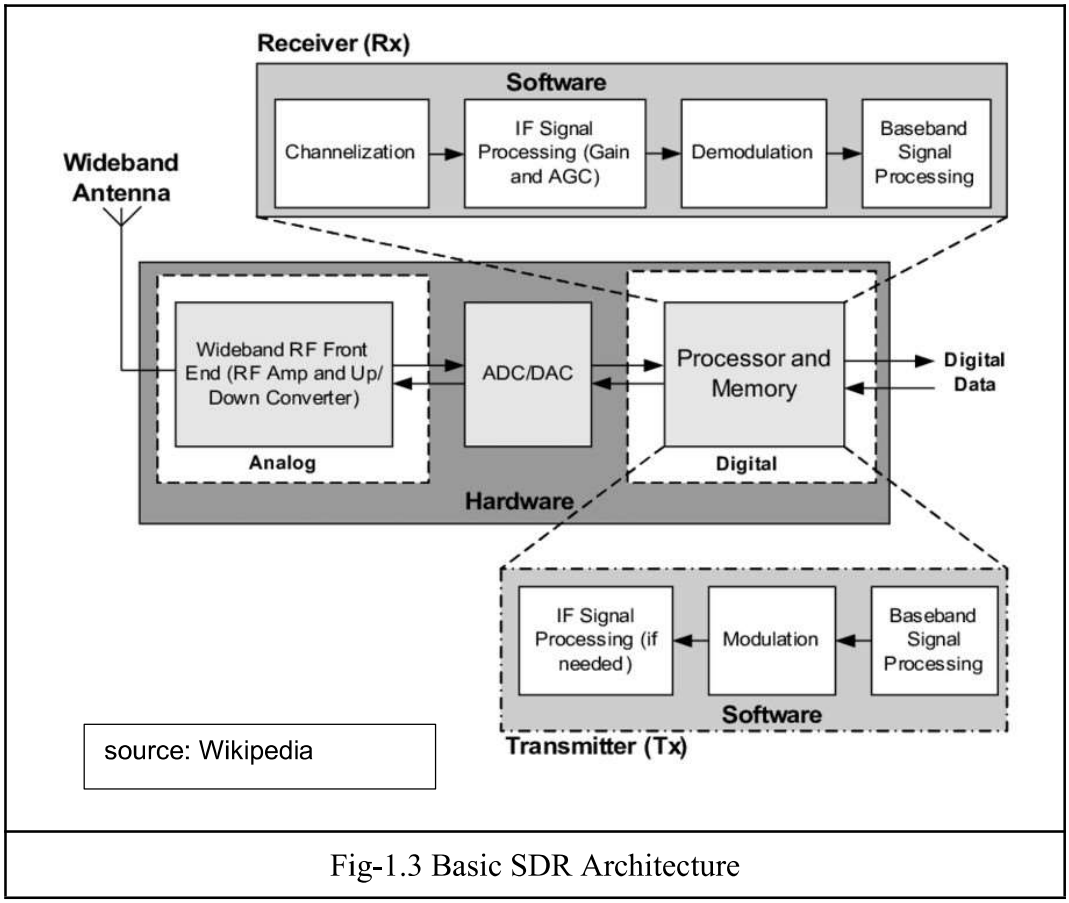

Fig-1.3 Basic SDR Architecture

The radio frequency (RF) signal is captured by an antenna, which is then amplified by a low-noise amplifier (LNA) to increase its strength. The signal is then mixed with a local oscillator (LO) signal to produce an intermediate frequency (IF) signal. All these things happen in the Analog front end shown in the figure.

The IF signal is then digitized using an analog-to-digital converter (ADC) and sent to a processor which is usually a digital signal processor (DSP) chip or an FPGA. The processor performs the signal processing tasks that would typically be done by analog circuits in a traditional radio receiver. The DSP can filter, demodulate, and decode the signal, as well as perform other advanced processing techniques such as noise reduction and equalization.

The processed digital signal or data is then sent to the computer or other digital computing device via a USB connection. The user can then use software to control the SDR and display the received signal on a screen. The software can also be used to decode various types of signals, such as FM radio, AM radio, digital TV, and more.

Chapter 2

SDR based Satellite Microwave Receiver

This chapter outlines a simple SDR based satellite receiver devised to receive microwave signals transmitted by any target satellite. In the process of setting-up this receiver several SDRs available in the lab tested, and finally HackRF-One SDR found to be most capable. Though the receiver is primarily set-up to receive a Ka-band beacon transmitted by ISRO's GSAT-14, it's found more of a use for receiving a Ku-band transponder signal meant for DTH broadcast, repurposed to check the water or rain-attenuation characteristics of the microwave signals. This receiver experiments were primarily motivated by an idea of utilizing the abandoned microwave receiver antennas at IIT Indore

2.1 Receiver Set-up for Ka-band Beacon Reception

A satellite beacon receiver is a type of radio receiver that is used to receive signals from satellites. These signals can be used for a variety of purposes, such as tracking the satellite's orbit or monitoring its health and status, and remote sensing applications. In recent years, software-defined radio (SDR) technology has become increasingly popular for satellite beacon receivers due to its flexibility and ease of use.

An SDR-based satellite beacon receiver typically consists of a computer, an SDR hardware device, and specialized software. The SDR hardware device is typically a USB peripheral that connects to the computer and provides the necessary radio frequency (RF) front-end for receiving signals from the satellite. The specialized software is used to control the SDR device and process the received signals.

One of the advantages of using an SDR-based satellite beacon receiver is that it allows for a wide range of signal processing options. The software can be configured to perform a variety of signal processing functions, such as filtering, demodulation, and decoding. This flexibility allows users to customize the

receiver for their specific needs and applications. Another advantage of SDR-based satellite beacon receivers is that they are relatively inexpensive and easy to use.

The experiment aimed to capture and record the Ka-band beacon transmitted by the GSAT-14 satellite of ISRO. The beacon receiver is a straightforward set-up that includes the outdoor Ka-band reflector antenna, a commercial Low-Noise Block down-converter (LNB), and a Software-Defined Radio (SDR) dongle that performs additional signal down-conversion and discretization before passing to a Personal Computer (PC).

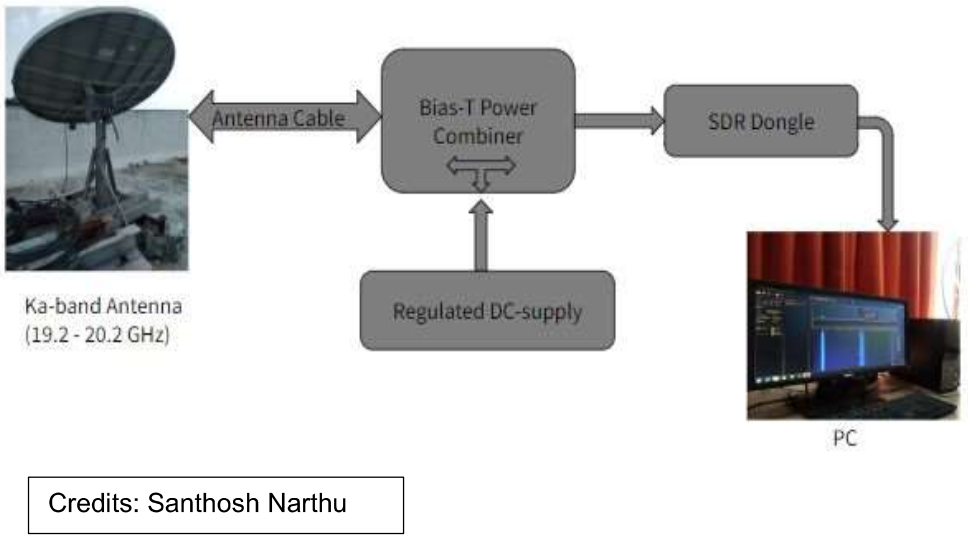

Fig-2.1 Receiver set-up for Ka-band beacon reception

The beacon receiver was set up using off-the-shelf components that were divided into two primary sections as follows.

2.1.1 The RF Outdoor Unit

The Ka-band dish and an LNB with a reliable local oscillator are part of the outdoor equipment. A 10 m low-loss coaxial cable is used to link the indoor unit to the LNB output connector (N-type 50). The LNB is likewise powered by 18 V

DC through the connection from the interior unit. The LNB provides low-noise amplification and block conversion to the common 0.950-1.950GHz IF over the original satellite RF frequency range 19.20–20.20GHz. This device has a noise figure of 1.3 dB and an overall gain of 55 dB, and L.O frequency of 18.25Hz

Fig-2.2 Out-door unit: Ka-band antenna with LNB

2.1.2 The Indoor Unit

This handles signal processing, a second frequency conversion, and data logging. It consists of an RTL SDR device connected to a PC. The computer performs data logging and signal processing. The RTL SDR is equipped with an RF transceiver that uses quadrature sampling and a second down-conversion. We set the SDR device to its lowest tunable bandwidth, 1.5MHz, to be roughly focused around the beacon frequency

2.1.3 SDR Software Installation and Testing

The SDR sharp software which is compatible with the RTL SDR used in the experiment is installed on the PC operating on Windows 10 OS.

The working of the software is tested by using a magnetic mount antenna available in the lab as a test antenna. Also the data logging functionality is checked on arbitrary frequencies which appeared prominent on the display, for instance FM signal as shown in Fig-2.4 below

a

b

@ Radio Wave Propagation Lab, IIT Indore

Fig-2.3 Indoor Unit

a

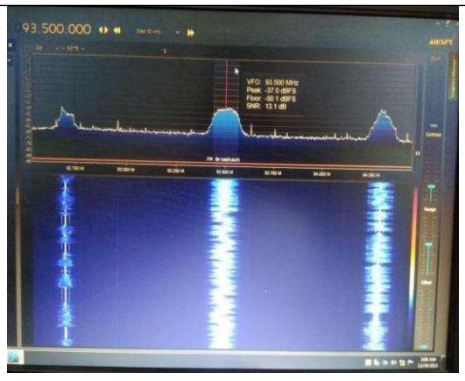

b

@ Radio Wave Propagation Lab, IIT Indore

Fig-2.4: SDR software installation and testing. Note: here 'Nooelec' SDR (black dongle in the left-side figure USB connected to CPU unit) was used

2.1.4 Antenna Adjustment and Beacon Reception

The Ka-band dish antenna, which was left unused, was initially at some random position as shown in the leftmost figure below. For establishing the required LOS with GSAT-14 the antenna on the workshop building is geolocated with its latitude and longitude coordinates (22 deg. 31.526 min North, 75 deg. 55.26 min. East), and subsequently the local azimuth and elevation angles are determined to be 185 deg. True North, 63.5 deg, respectively. The rightmost figure below shows the actual positioning upon which the beacon is received.

2.1.5 Ka-band Observations

Fig-2.6 shows how the strength of the beacon is improved with tuning of elevation angle to the required 63.5 deg. The rightmost figure shows the beacon with the highest possible strength of reception which was found to be 25 dBm above the noise floor on the scope of the spectrum analyzer used for testing purposes.

Fig-2.5 Ka-band antenna adjustment

The beacon was successfully received at 1.728 GHz of down converted frequency that corresponds to the 19.978 GHz frequency of the actual Ka-band beacon transmitted by GSAT-14. As seen in the figure (b) the signal strength on the

spectrum analyser was found to be -66.2 dB with a gain of around 25dBm over the noise floor. This signal received at the 1.728GHz which corresponds to 19.978 GHz well in the 19.20 - 20.20 GHz frequency range of the Ka-band LNB. But the

signal is also found to be very transient and not consistently present. The same can be observed in The Fig-2.6.2 which shows a one day record of the signal

a

b

Fig-2.6.1 Reception of Ka-band reception

after replacing the spectrum analyser with the SDR (HackRF-One). But this signal power over noise level is very low (-4dBm) when compared to -25dBm with a spectrum analyser. This raised a suspicion about the SDR based receiver in this case, so subsequently I experimented more to see if it actually works by testing it with another antenna which receives Ku-band microwave signals. This is explained in the following section.

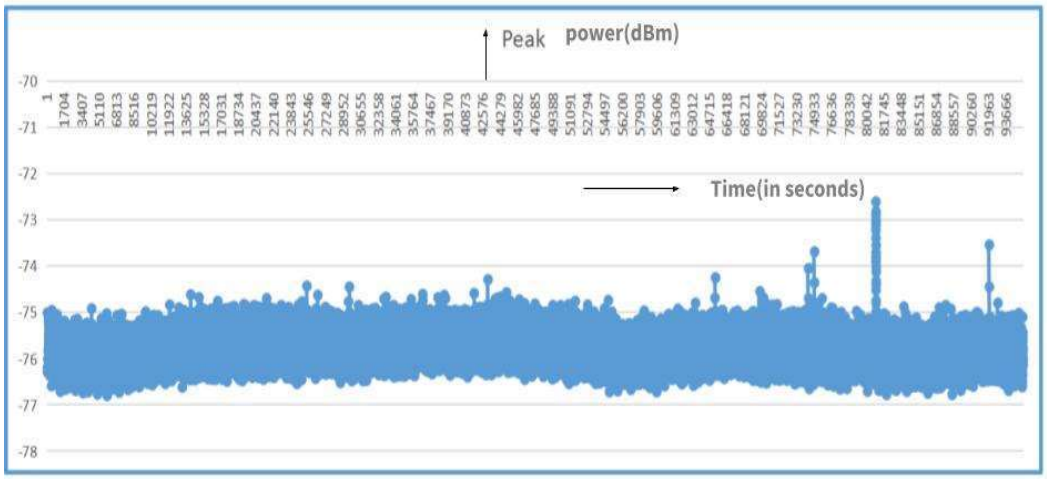

Fig-2.6.2 Ka-band signal(beacon) record using the SDR in place

2.2 Ku-band Reception and Data Logging

The same Receiver is now used with another antenna that receives 10.70 - 12.75 GHz frequencies that fall in the bottom edge of the Ku-band. This time, in the receiver set-up the spectrum analyser is initially used to view the signal received in the Ka-band. Fig-2.7 shows all the equipment in the receiver chain and the spectrum of the signals which are basically satellite transponder signals meant for DTH video broadcasting. The specifications of the LNB shown in the figure are as follows, input frequency: 10.70 - 12.70GHz, output frequency: 950-2150MHz, L.O(local oscillator frequency): 9.75/ 10.6GHz, Noise: 0.1dB

Later the spectrum analyser is replaced with the HackRF-One which is capable of receiving signals up to 6 GHz range, with a sampling rate of 20Msps (i.e., it supports signal bandwidth of up to 10MHz for the real signals). Fig-2.8 shows the HackRF-One powered and connected in receive mode with SDR sharp software. The receive mode is indicated by the top LED which is glowing yellow near the transceiver port on right side and that is basically SMA connector

The Fig-2.9 shows the receiver for the Ku-band with the HackRF-One tuned in software (GUI interface of the SDR sharp) to 2.090 GHz as visible on the laptop screen in the figure. Not so clearly visible but the signal peak power at this frequency is around -60dBm with the HackRF's bandwidth set to 1MHz and its amplifiers both LNA and VGA set to -24dB gain. These gain values can be set to any number that can give a reasonable strength to the signal of interest. In order to check the signal response to the water or rain, the Ku-band antenna is obstructed with water. This is also shown in the Fig-2.9 on its right side

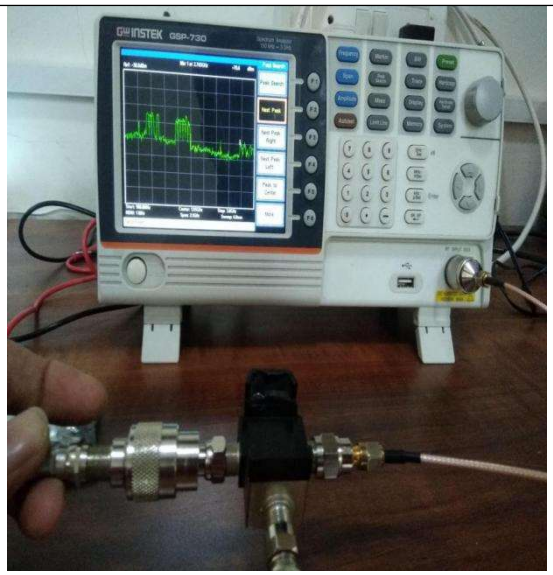

a

@ Radio Wave Propagation Lab, IIT Indore

b

c

Fig-2.7 Ku-band reception with spectrum analyser
a). Indoor set-up, b). Ku-band antenna c). LNB for Ku-band

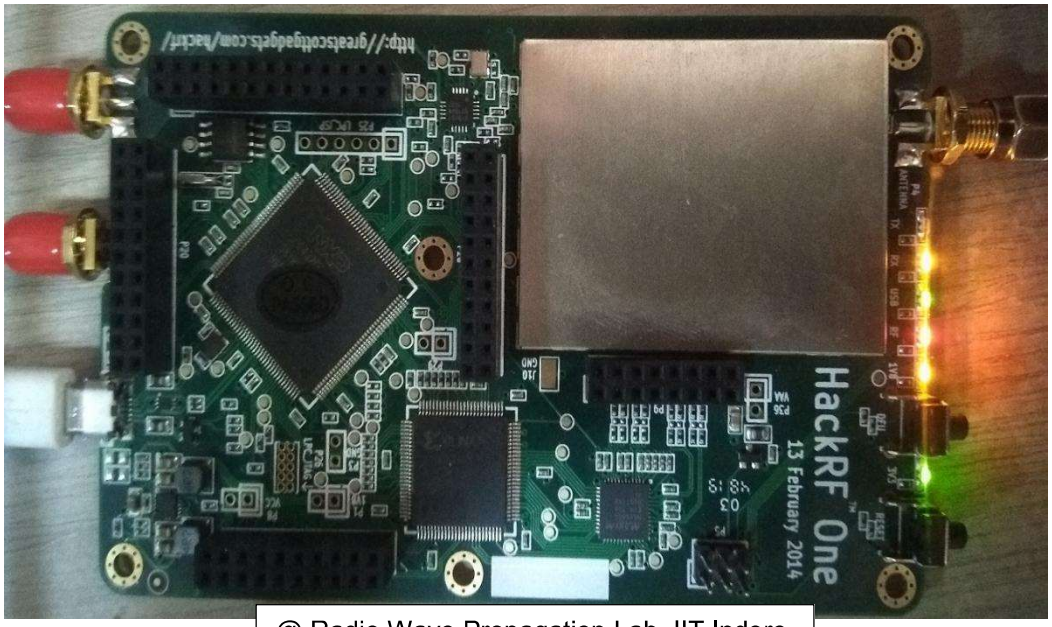

@ Radio Wave Propagation Lab, IIT Indore

Fig-2.8 HackRF-One powered, connected in Receive mode

a b

@ Radio Wave Propagation Lab, IIT Indore

Fig-2.9: HackRF-One Receiver for Ku-band signal logging (left), the receiver antenna obstructed with a volume of water (right)

2.2.1 Ku-band Observations and Results

The Fig-2.10 shows the water absorption characteristic of the Ku-band at two different frequencies. The details of the signal frequencies and the corresponding power levels are shown in Fig-2.11 along with the exact values listed in Table-2.1.

Table-2.1 Signal attenuation with water

Frequency (GHz)	**Peak power (dBm)**	
10.83	-40	-47.3
12.68	-53.5	-57.5

The frequencies listed as 10.83GHz and 12.68GHz are obtained by up-converting the actual values set or tuned with the HackRF-One which are 1.080GHz, and 2.080GHz respectively. These values are chosen with the help of a previous observation with the spectrum analyzer, which is shown in Fig-2.12. The figure shows two bands of transponder signals, one centered around 1GHz (10.75GHz up-converted with L.O. 9.75GHz), and the other centered around 2GHz (12.60GHz up-converted with L.O. 10.60GHz).

2.2.1.1 More Interesting Observation

The HackRF One based receiver is working very well with a full capability of continuous data. The Fig-2.13 shows an interesting observation that can offer a potential chance to infer some remote sensing information of the atmosphere on interaction with these microwave frequencies. This is observed on one of the transponder signal carriers where it's exhibiting some kind of repeating response over time. Interestingly the dips in the peak power level is observed during the daytime. Fig-2.14 shows the zoomed out view of one of these dips that shows a drop in signal level of 2 to 3 dBm, which is significant. Note: a strong and sudden drop of signal level in the fifth dip is due to the water obstruction experiment done on that day around 10.30a

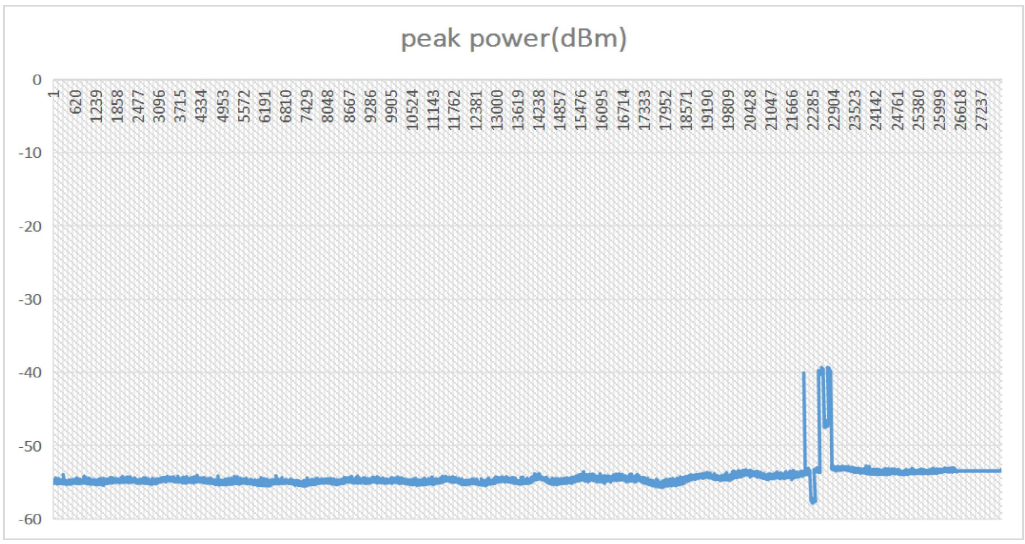

Fig-2.10 Signal attenuation due to absorption by water (Ku-band)
X:axis: peak power(dBm), Y:axis: time(in seconds)

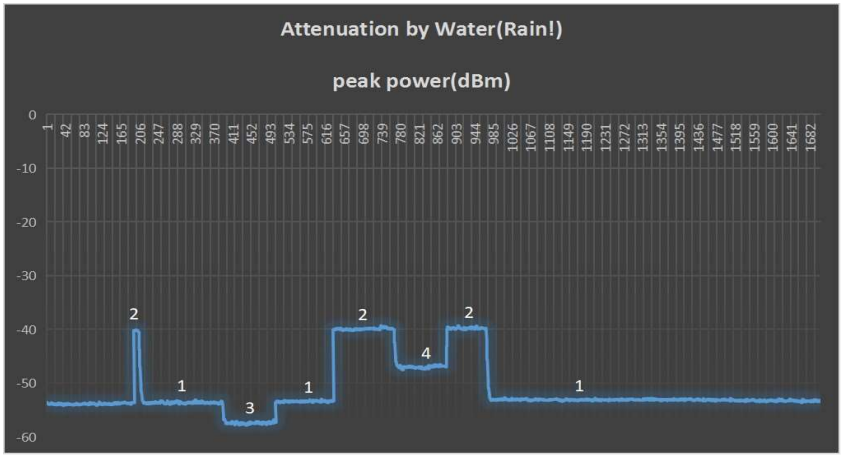

Fig-2.11 Attenuation levels over two different Ku-band frequencies
X:axis: peak power(dBm), y:axis: time(in seconds)

1. -53dBm
2. -40dBm
3. -57.5dBm
4. -47.3dBm

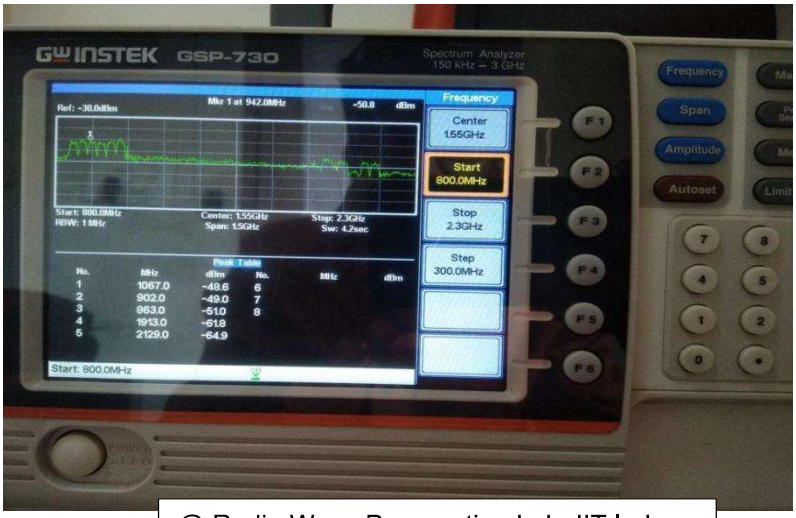

@ Radio Wave Propagation Lab, IIT Indore

Fig-2.12 Detailed observation of the Ku-band transponder signals on spectrum analyser

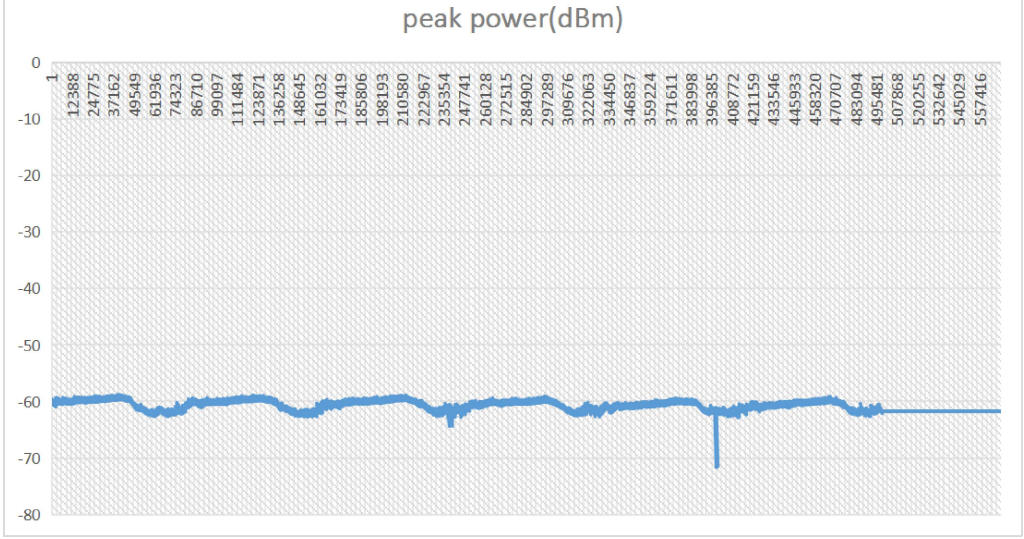

Fig-2.13 an interesting signal pattern observed over a period of 6 days\
X:axis: peak power(dBm), y:axis: time(in seconds)

The capability of the receiver to record the signal level over several days can be utilized to study remote sensing parameters like atmospheric moisture content, cloud cover, temperature profile etc.

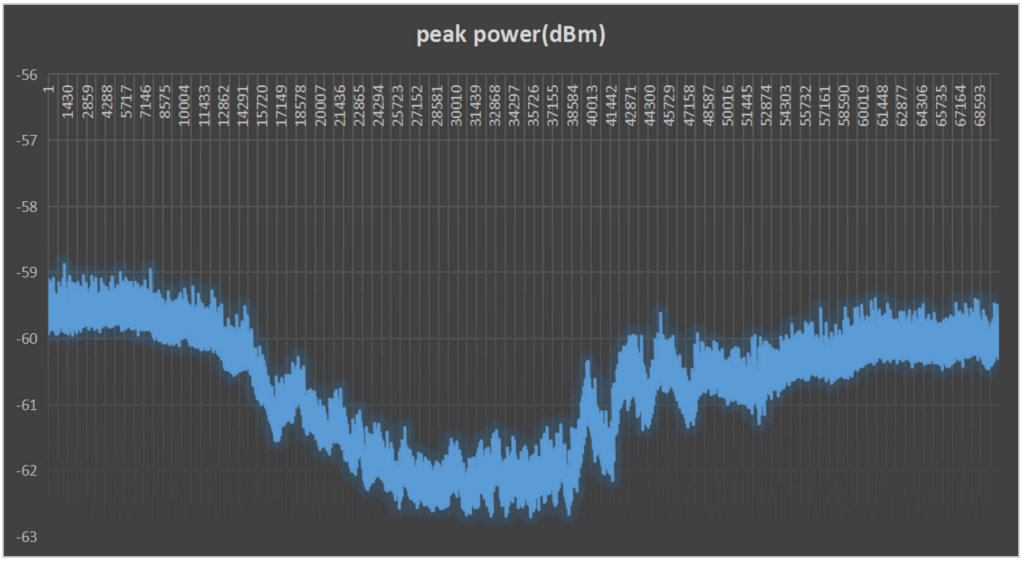

Fig-2.14 Detailed view of the dip on the second day
X:axis: peak power(dBm), y:axis: time(in seconds)

Table-2.2 Cost of the Receiver-1

S.No	Equipment	Quantity	Price per unit (₹)	Total Price (₹)
1.	Bias Tee	1	1,500	1,500
2.	Coaxial Cables	2	250	500
3.	RP SMA Connector	1	500`	500
4.	DC Power adapter	1	750	750
5.	SDR (RTL SDR/ HaackRF-One)	1	5,000 - 30,000	5,000 - 30,000
Grand Total				**8,250 - 33,250**

The receiver used HackRF-One SDR which is a bit costly, and has far more capabilities than what is just needed in this application. So, it's possible to replace this SDR with lower cost SDRs which are readily available in the market. The Table 2.2 shows the cost estimation of the receiver system with respect to the use of both HackRF-One and a typical lower cost SDR.

Chapter 3

Development of Low-cost GNSS-IR Sensor for Soil Moisture

3.1 Literature Review

The understanding of land-surface parameters is extremely important for climate change and weather impacts, particularly the influence of soil moisture content (SMC) on hydro-meteorological and ecological processes. Volumetric soil moisture, or the ratio of the volume of water to the volume of soil, is currently estimated using both in situ and remote sensing techniques. Unfortunately, in situ measurement methods are expensive and cumbersome over large areas, whereas measurements from satellite active and passive microwave sensors have shown advantages for SMC monitoring. Recently, new methods of utilizing the signals of opportunity from Global Navigation Satellite Systems (GNSS) have been emerging. This technique is broadly known as GNSS-Reflectometry, which offers wide applications in Earth's surface remote sensing due to its numerous advantages like: quick revisiting time, global coverage, low cost, all-weather, and near real-time when compared to conventional observations

The GNSS-Reflectometry can be broadly divided into two categories. The first one uses a receiver with at least two antennas to detect direct and reflected signals separately of a particular GNSS satellite, sometimes called GNSS-R method. This uses the dielectric method to convert the $\in$ to SMC through the dielectric mixing models. With this method the receiver can be in situ, on aircraft or satellite borne. The second method uses classical GNSS receivers with only one antenna and it is only applicable in situ and low-altitude flights. To estimate the SMC values this method uses either the interference diagram or the SNR amplitude, and is usually called GNSS-IR (interferometric reflectometry).

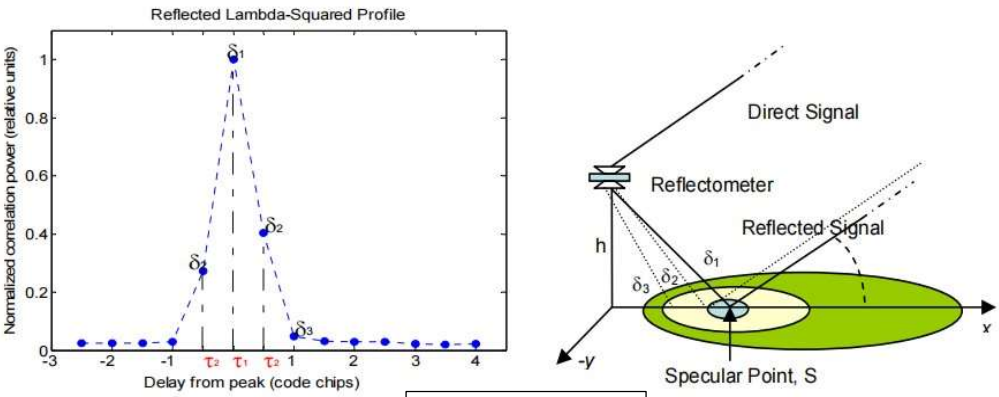

Fig-3.1 GNSS-R working principle

The figure on the left below shows the interference of direct and reflected signals, and on the right is the SNR pattern as the satellite flys through the sky having different elevation angles. The waggles in the SNR at raising and setting phases of the satellite is of our use for estimating soil moisture with GNSS-IR technique.

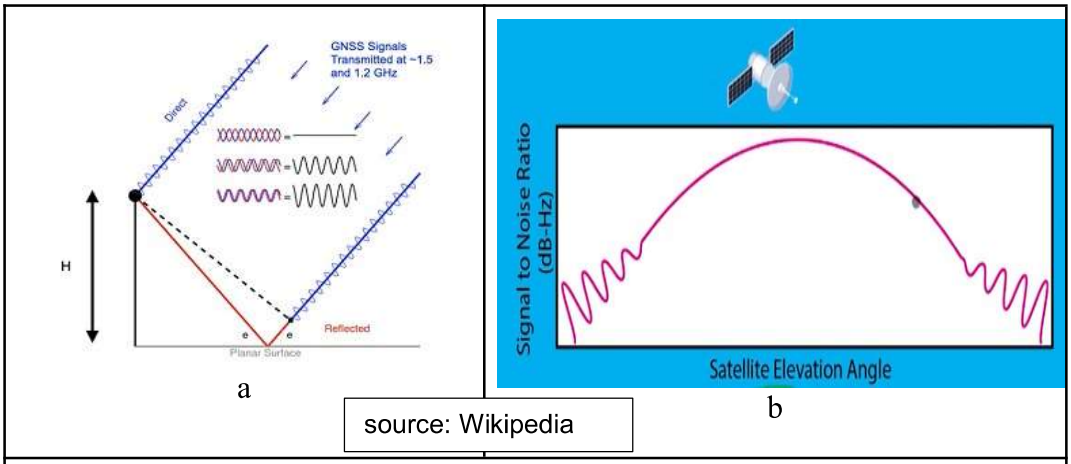

Fig-3.2 (a) GNSS-IR working principle, (b) SNR pattern of the received signal

The focus of this work is on GNSS-IR instrumentation which is relatively less complex, and has more utility

3.1.2 GNSS-IR Methodology for Estimating Soil Moisture

The conceptual time series of SNR data which is shown as a function of elevation angle in the last figure is a combination of both direct and the interference between direct and reflected signals. The direct signal can be approximated as a parabolic function as shown in the middle of the below figure. It would be a lot simpler if we remove the direct signal component from the SNR data. After it's subtracted out it looks like what is shown in the bottom of the figure, which would just represent the interference between the direct and reflected signals, and is often termed as interferogram. The middle part of this pattern doesn't contain any data, and we're only interested in the waggles at the beginning and end of that pattern

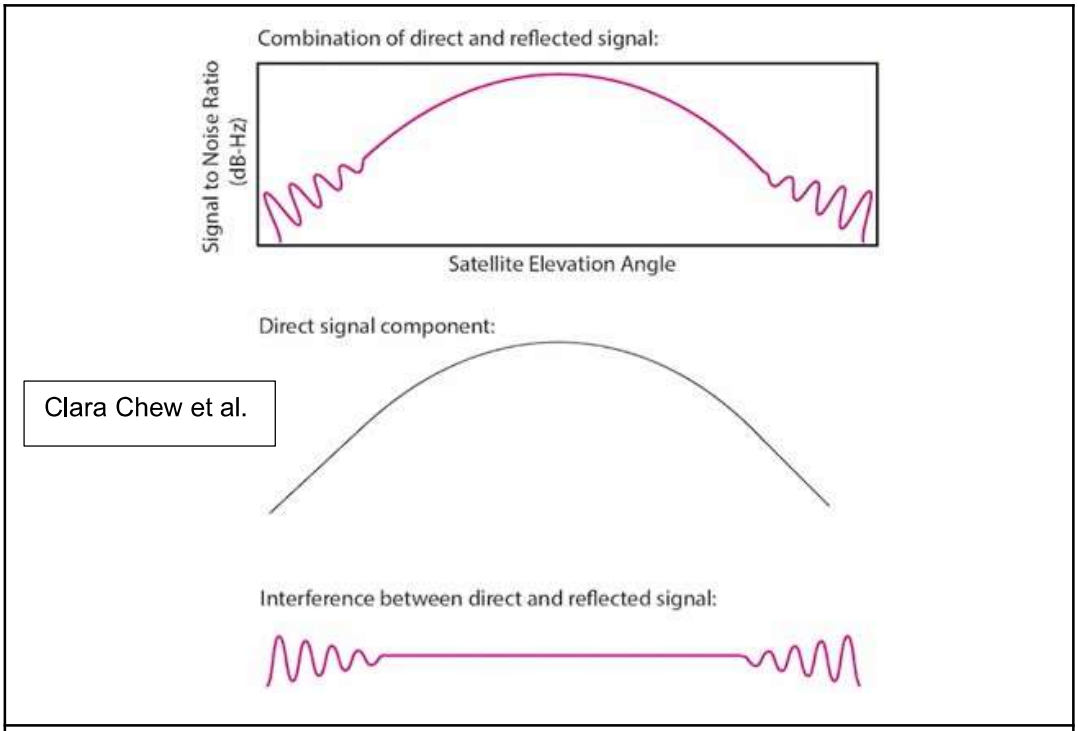

Fig-3.3 Direct and Interference signals of the received signal

The following figure shows a typical SNR interferogram recorded from a high quality GNSS receiver. The interferogram changes with what is in the vicinity of the antenna site, for example, the soil moisture, vegetation cover, and snow etc.

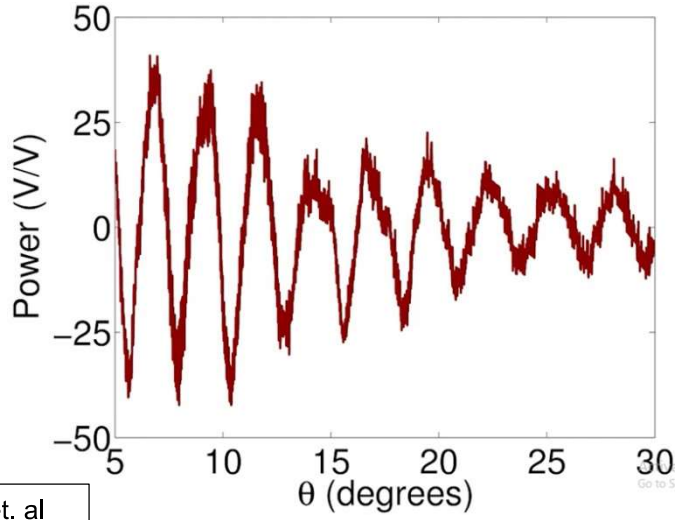

Fig-3.4 A typical SNR interferogram

Usually, just looking at the SNR interferograms themselves and figuring out how the parameters like soil moisture change over time is hard. For example, below are two interferograms from the GNSS antenna that were recorded before and after a rein event. They are a little different, but it's not super obvious how they're different and further the noise in the interferogram seems to get in the way.

Now it's common in GNSS-IR that these interferograms are modeled with the following standard equation, which is sine curve as a function of elevation angle, with amplitude *A,* a frequency term, and phase offset ϕ

$$SNR = A\cos\left(\frac{4\pi H_0}{\lambda}\sin\theta + \phi\right)$$

The three parameters are often called SNR metrics, and are estimated by fitting each of the interferograms to the above equation. The λ in the above equation represents the wavelength of the GPS/GNSS signal

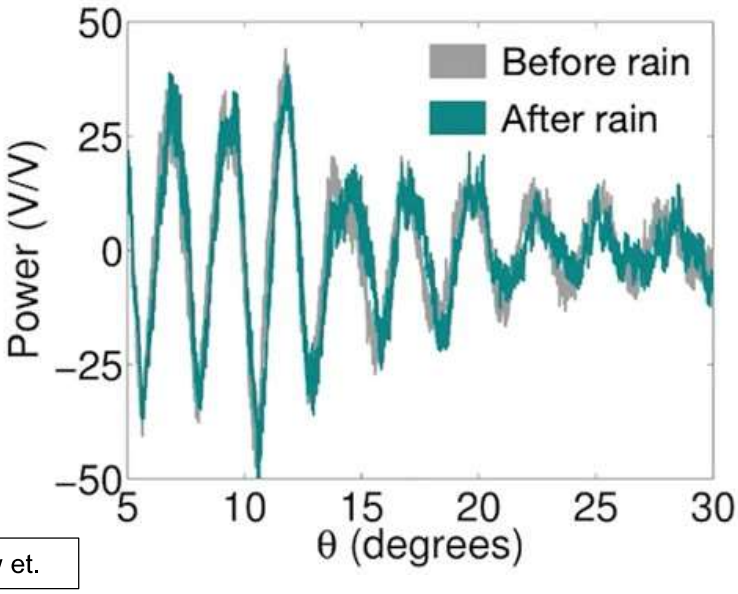

Fig-3.5 Change in interference pattern on rain event

The following shows such a fitting of interferograms to the SNR equation, and the conceptual view of corresponding changes in amplitude and phase separately. Larger amplitudes correspond to lower elevation angles, and the change in phases just tells how interferograms shift back and forth in time. The frequency term is a more complicated term which is of use in finding the effective reflector height *H,* which is of no concern estimating soil moisture content.

From the above illustration we can see that the increase in soil moisture from the rain causes a slight decrease in amplitude and small phase offset as well. We can make a time series of the phase offset which is going to be different each day and

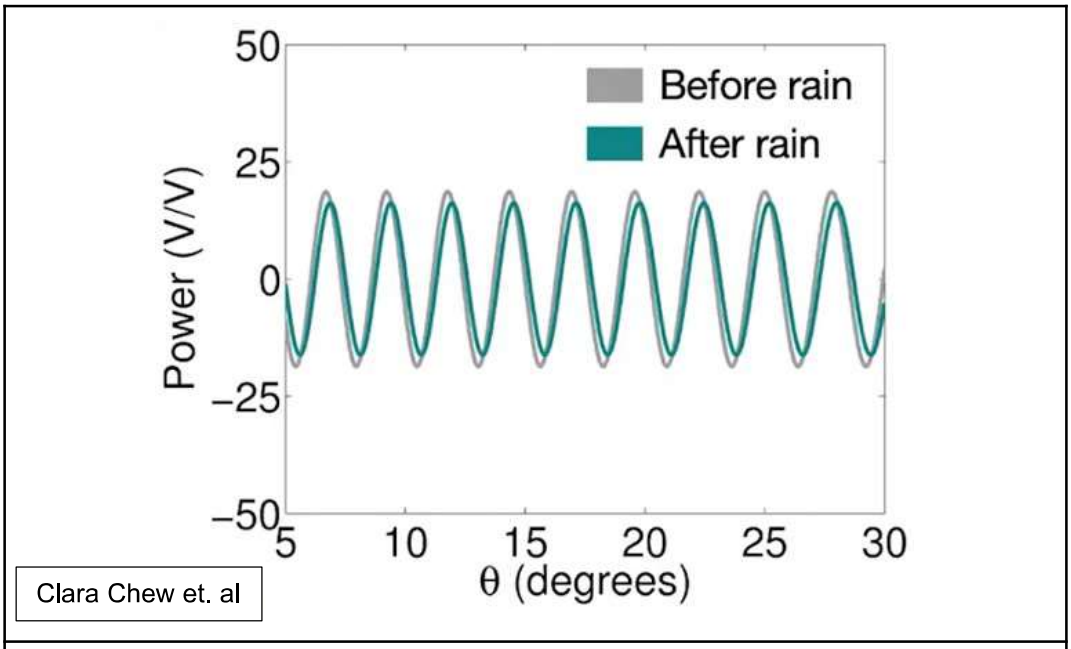

Fig-3.6 Interferograms fitted to SNR characteristic equation

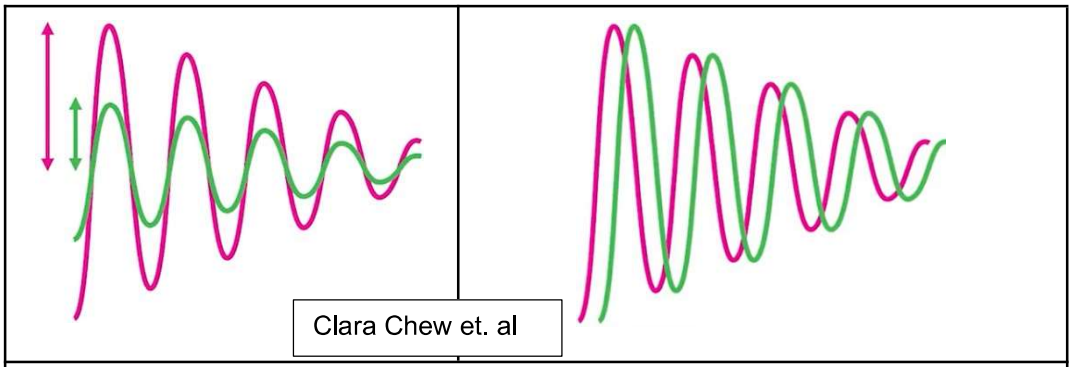

Fig-3.7 Amplitude, and phase effects with change in soil moisture

compare it with a time series of soil moisture measured at the same antenna where the SNR data is being recorded. The Fig-3.8 shows such measurements. The figure at the top shows soil moisture as a function of time which is recorded by a soil moisture probe commercially available. It shows a sudden raise in soil

moisture content around day 253, which can also be clearly seen in the bottom time series plot derived from SNR data.

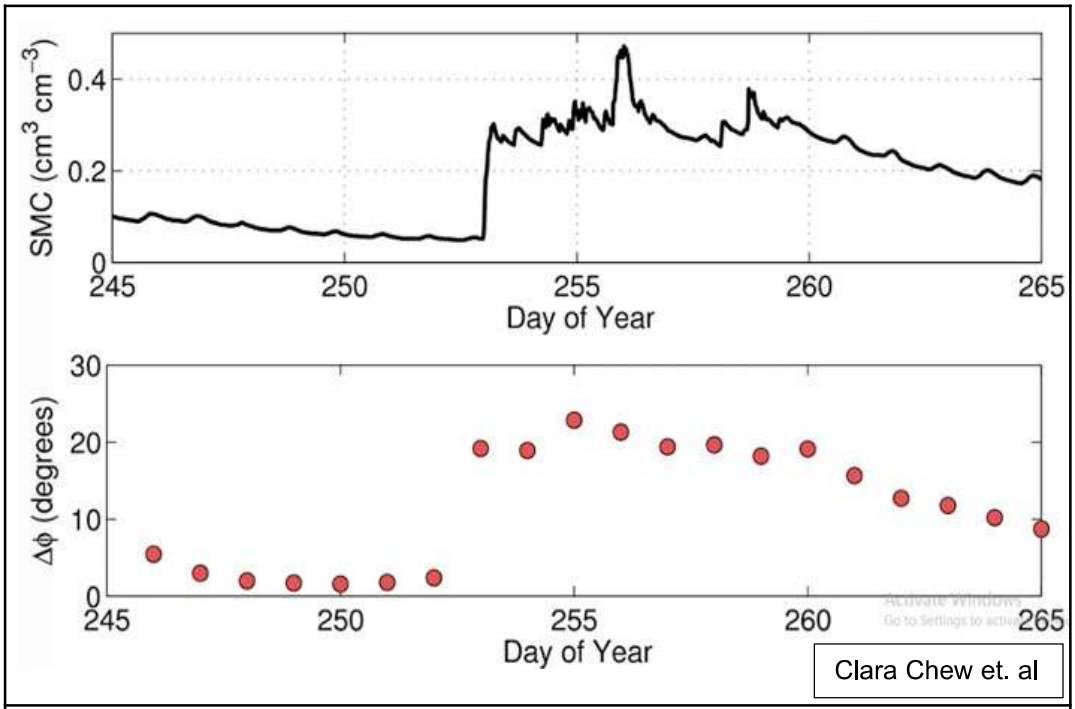

Fig-3.8 Correlation between soil moisture and change in phase offset

Similarly both the plots show a slow decline starting from day 260. This empirically proves a strong correlation between the phase and soil moisture. If we see an increase in the phase of the SNR data with time then we can assume that there has also been an increase in soil moisture in the vicinity of the GNSS antenna

3.1.3 Existing GNSS-reflectometry Instrumentation for Soil Moisture

The following figure shows one of the receiving stations of the PBO(Plate Boundary Observatory) network in the USA which is repurposed to measure soil moisture of the surface in its vicinity. But these are very costly receiving stations meant to accurately measure the Earth's tectonic plate movements. The figure

shows the campaign kit provide by UNAVACO, and the site of actual PBO receiver station

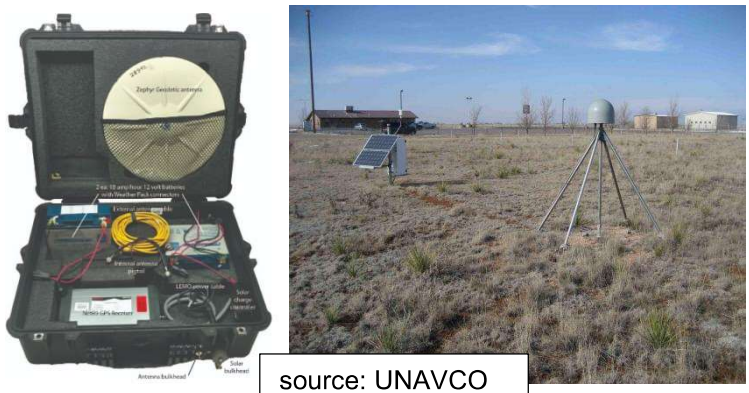

Fig-3.9 PBO station repurposed to soil moisture monitoring

There have been so many efforts to develop different sensors specifically for monitoring soil moisture using GNSS reflectometry, the Fig-3.10 shows such instrumentation. The first figure shows GNSS-R instrumentation which uses separate receiver set-ups to receive direct (a), and reflected signals (b) independently, and continuous recording of soil moisture using a soil-moisture probe (c). The second figure shows GNSS-IR campaign for soil moisture that directly installs a ready made kit.

3.2 Opportunity for a Low-cost Design

For more than a decade GNSS-IR (interferometric reflectometry) evolved as a standard remote-sensing method for estimating geophysical parameters like soil moisture, vegetation water content, ice-sheet thickness etc. GNSS-IR uses GNSS signals as signals of opportunity, which are everywhere on earth like sun-rays. We even have a network of GNSS-IR receivers [PBO network, USA] for soil moisture, but they are actually the high cost, high quality geodetic receivers repurposed for soil moisture monitoring. Here, the important observation is these quality receivers are meant to reject multipath, but still they supported GNSS-IR which is based on multipath reception.

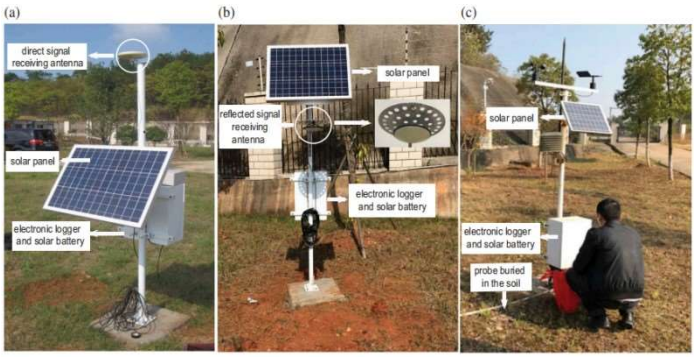

a

Xing Chang et. al

b

Xing Chang et. al

Fig-3.10 (a) GNSS-R instrumentation (S. Yan Et. al), (b) GNSS-IR instrumentation ((Xin Chang Et al), for soil moisture

This places a huge opportunity for a dedicated design of the GNSS-IR receiver for soil moisture, which has lot of scope to be cost-effective making very low-cost antennas usable for more multipath reception, and potentially better soil moisture estimates

3.3 Testing the suitability of a Low cost GNSS receiver (Ublox) for use in GNSS-IR

To ensure that a low cost GNSS receiver like u-blox can be used to generate the required SNR pattern for subsequent estimation of soil moisture using GNSS-IR,

the receiver is tested in the laboratory and it's found that it's capable. The result (Fig (c)) in the following figure illustrates this

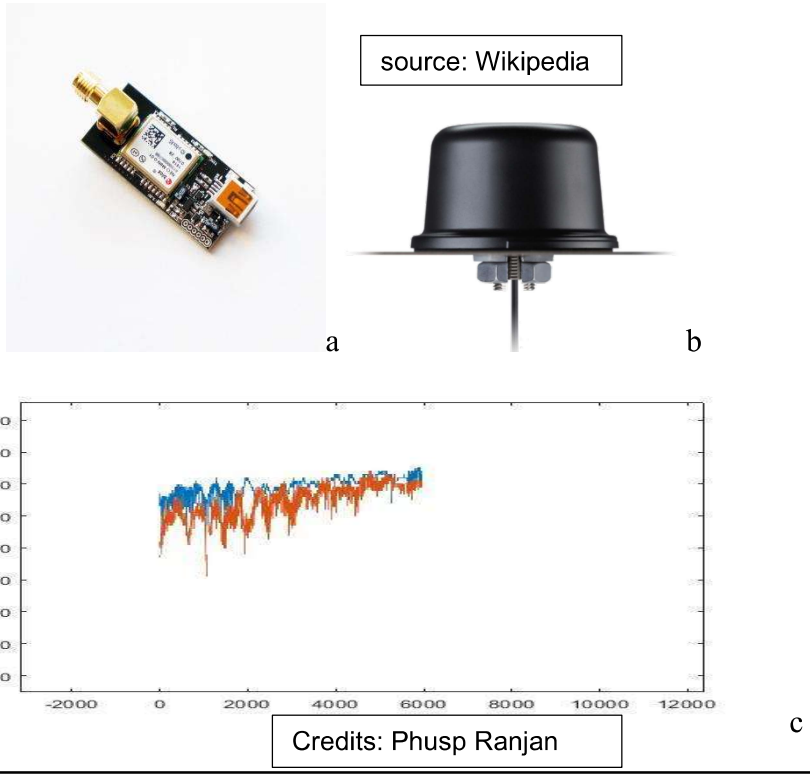

Fig-3.11 (a) u-blox receiver (b) Taoglas GNSS antenna (c) SNR pattern obtained by the u-blox receiver in lab **(x-axis: Time epoch (in seconds)), y-axis: SNR))**

And further, the antenna (GNSS multiband) used here, which costs around Rs. 15000, can be replaced with any single frequency GNSS receiver and can further bring down the cost of the entire system to a very low price.

3.4 GNSS-IR Sensor Design

With the encouraging results obtained in the above section, a system design shown in Fig-3.13 made out of the understanding from the literature review of the GNSS-IR instrumentation related to soil moisture estimation, is proposed for probable creation of a low-cost sensor.

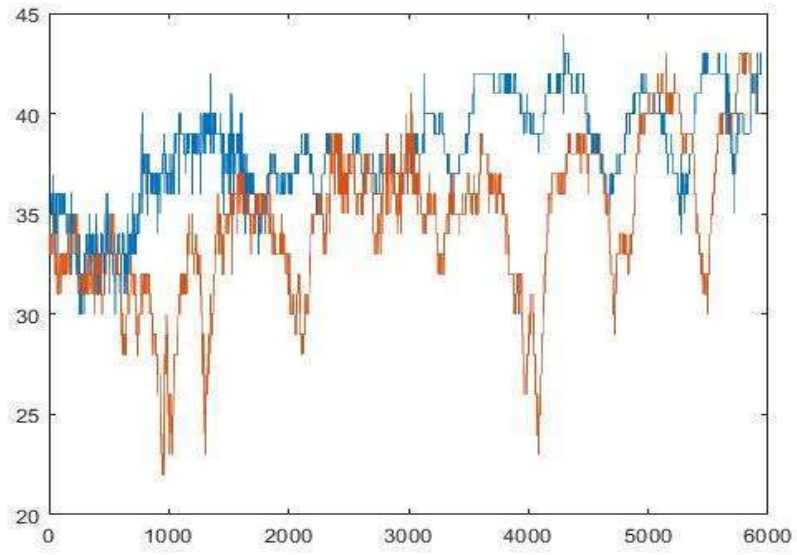

Credits: Phusp Ranjan

x-axis: Time epoch (in seconds)), y-axis: SNR

Fig 3.12 SNR Interferogram (enlarged view)

3.4.1 Sensor Integration with the actual equipment in Lab

Simpler consumer-grade GPS/GNSS receivers that merely output SNR can be used. In contrast, professional equipment produces measurements using the pseudorange and carrier phases, which is not of any concern in estimating soil moisture is not needed here. So with a prime focus on reducing the GNSS receiver cost the following is the list of components used in the attempt to build the system.

List of components used:

- u-blox GNSS receiver
- Taoglas GNSS antenna(s)
- Raspberry Pi 3
- Powerbank for power supply

- USB connectors
- 3-D printed box

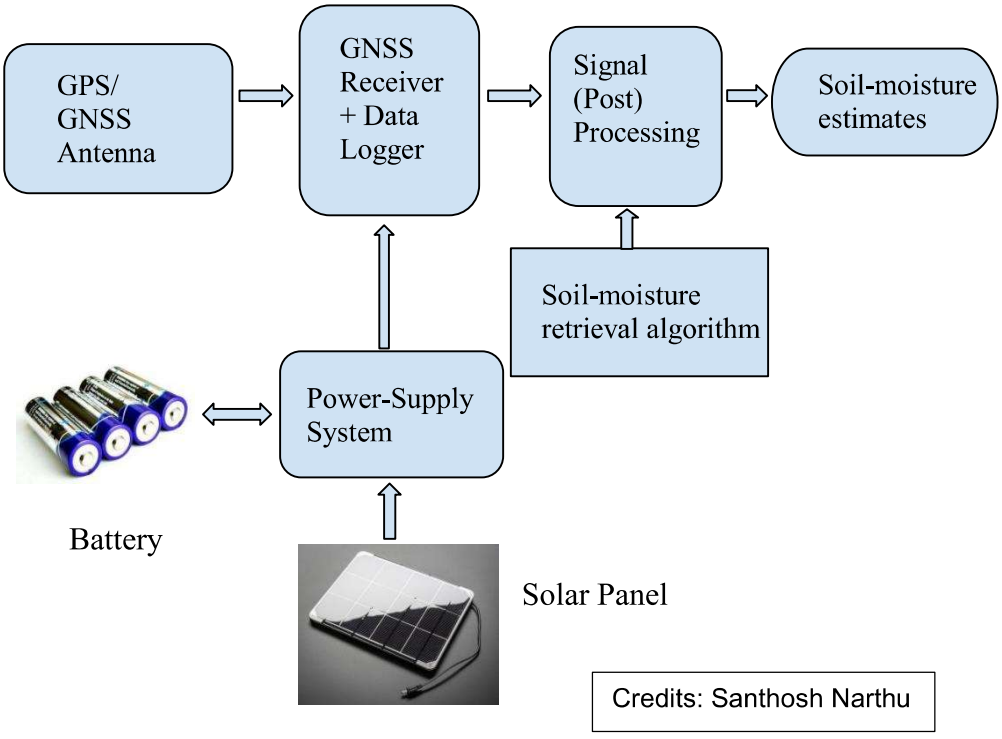

Fig-3.13 GNSS-IR System Block diagram

The Figures 3.14 shows the creation of the prototype. This prototype exhibited successful functionality in the lab, receiving signals from multiple constellations on L1 and L2 frequencies with the desired SNR values. However, when taken into the field, the receiver encountered challenges primarily caused by heating issues with the Raspberry Pi. As a result, we faced difficulties in fully operationalizing the system during the final phase where it needs to be employed for the field campaign. Nonetheless, further experimentation and refinement of the instrumentation offer potential for overcoming these challenges and realizing a low-cost, fully functional system for soil moisture estimation.

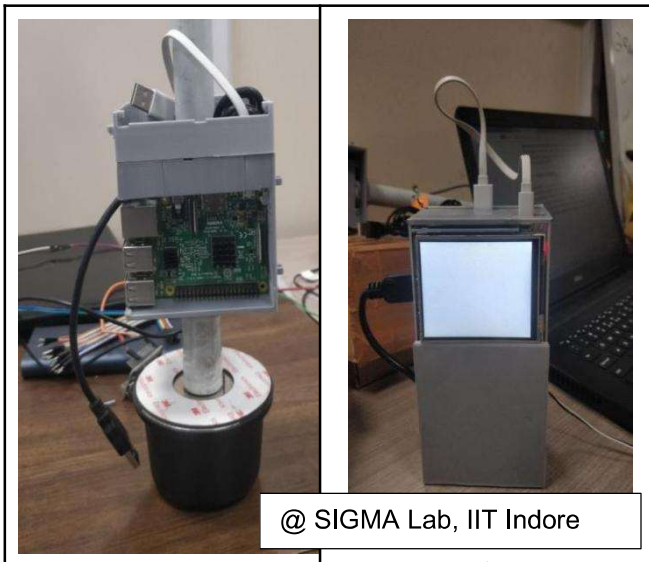

a b c

Fig-3.14 (a), (b) Sensor integration, (c) Final Prototype for field campaign (actually two prototypes, one with smaller low-cost antenna, the other with higher quality antenna)

Table-3.1 enlists the details of the cost of this system prototype.

Table-3.1 Cost of the Receiver-2

S.No	**Equipment**	**Quantity**	**Price per unit (₹)**	**Total Price (₹)**
1.	u-blox GNSS receiver (ZED-F9P type)	1	3,000	3,000
2.	Taoglas GNSS antenna	1	15,000	15,000
3.	Raspberry Pi 3	1	5,000	5,000
4.	Power Bank	1	800	800
5.	3-D printed enclosure	1	200	200
Grand Total				**24,000**

Chapter 4

Conclusion

This work encompasses my endeavors put in devising two distinct satellite-microwave receiver systems intended for remote sensing applications.

With the first system which is the SDR based receiver, I achieved success in implementing a complete functionality for signal reception and data recording of signal power levels, and this makes it a fully functional Satellite-Microwave receiver. This type of receiver can facilitate the inference of rain-fade characteristics, extraction of remote sensing information pertaining to the atmosphere, or can be used for any other potential applications that involve microwave signal reception.

For the GNSS based receiver, our progress was promising up until the prototype development stage; however, we encountered difficulties in fully operationalizing the system during the final phase. Further experimentation and refinement of the instrumentation are required to transform this opportunity into a fully functional systems for soil moisture estimation

REFERENCES

1. Low-Cost *Ka*-Band Satellite Receiver Data Preprocessing for Tropospheric Propagation Studies Vicente Pastoriza-Santos 1,* , Fernando Machado 1 , Dalia Nandi 2 and Fernando Pérez-Fontán 1
2. Larson K. M. and S. Miyazaki, Resolving Static Offsets from High-Rate GPS Data: the 2003 Tokachi-oki earthquake, *Earth, Planets, Space*, 60, 801-808, 2008
3. Soil Moisture Remote Sensing: State-of-the-Science Binayak P. Mohanty, Michael H. Cosh, Venkat Lakshmi, and Carsten Montzka, 2017
4. Soil Moisture Estimation by GNSS Multipath Signal, Xin Chang , Taoyong Jin, Kegen Yu, Yunwei Li , Jiancheng Li and Qiang Zhang , 2019
5. Chew, C., R. Shah, C. Zuffada, G. Hajj, D. Masters, and A. J. Mannucci. 2016a. "Demonstrating Soil Moisture Remote Sensing with Observations from the UK TechDemoSat 1 Satellite Mission." Geophysical Research Letters 43 (7): 3317–3324.
6. Chew, C., E. E. Small, and K. M. Larson. 2016. An Algorithm for Soil Moisture Estimation Using GPS interferometric Reflectometry for Bare and Vegetated Soil. GPS solutions 20 (3): 525–537.
7. Katzberg, S. J., et al, ''Utilizing Calibrated GPS Reflected Signals to Estimate Soil Reflectivity and Dielectric Constant: Results From SMEX 2,'' *Remote Sensing of Environment 100,* 17-28, 2005.
8. Larson, K.M.; Small, E.E.; Gutmann, E.; Bilich, A.; Axelrad, P.; Braun, J. Using gps multipath to measure soil moisture fluctuations: Initial results. *GPS Solut.* 2008, *12*, 173–177.
9. Larson, K.M.; Braun, J.J.; Small, E.E.; Zavorotny, V.U.; Gutmann, E.D.; Bilich, A.L. Gps multipath and its relation to near-surface soil moisture content. *IEEE J. Sel. Top. Appl. Earth Obs. Remote Sens.* 2010, *3*, 91–99.
10. Using reflected signal power from the BeiDou geostationary satellites to

estimate soil moisture SongHua Yan, Nan Zhang, NengCheng Chen & JianYa Gong , 2018

11. An open-source low-cost sensor for SNR-based GNSS reflectometry: design and long-term validation towards sea-level altimetry, M. A. R. Fagundes1 · I. Mendonça-Tinti2 · A. L. Iescheck3 · D. M. Akos4 · F. Geremia-Nievinski
12. Chen Q (2016) Optimization of GPS interferometric reflectometry for remote sensing. PhD thesis, University of Colorado Boulder
13. Larson KM, Small EE (2016) Estimation of snow depth using L1 GPS signal-to-noise ratio data. IEEE J Sel Top Appl Earth Obs Remote Sens 9(10):4802–4808
14. Larson KM (2016) GPS interferometric reflectometry: applications to surface soil moisture, snow depth, and vegetation water content in the western United States. Wiley Interdiscip Rev Water 3(6):775–787
15. Roesler C, Larson KM (2018) Software tools for GNSS interferometric reflectometry (GNSS-IR). GPS Solut 22(3):80
16. Utilizing Calibrated GPS Reflected Signals to Estimate Soil Reflectivity andDielectric Constant: Results from SMEX02 Stephen J. Katzberg*, Omar Torres*, Michael S. Grant* and Dallas Masters *NASA-Langley Research Center Hampton, VA 23
17. Katzberg S, Torres O, Grant M, Masters D (2006) Utilizing calibrated GPS reflected signals to estimate soil reflectivity and dielectric constant: results from SMEX02. Remote Sens Environ 100(1):17–28
18. Masters D, Axelrad P, Katzberg S (2004) Initial results of land-reflected GPS bistatic radar measurements in SMEX02. Rem Sens Envir 92(4):507–520
19. Teuling AJ, Seneviratne S, Williams C, Troch P (2006) Observed timescales of evapotranspiration response to soil moisture. Geophys Res Lett, 33(23), doi:10.1029/2006GL028178
20. Ulaby F, Moore R, Fung A (1986) Microwave remote sensing, active and passive, vol. III: from theory to applications. Artech House, Norwood

Some Useful Web-links:

- https://www.rtl-sdr.com/rtl-sdr-quick-start-guide/
- https://www.rtl-sdr.com/sdrsharp-users-guide/
- https://www.tylerwatt12.com/tips-for-using-sdr/
- https://greatscottgadgets.com/sdr/
- https://www.unavco.org/data/gps-gnss/derived-products/pbo-h2o/documentation/documentation.html#soil
- https://github.com/kristinemlarson/gnssrefl
- https://gnssrefl.readthedocs.io/en/latest/pages/README_vwc.html